PERGAMON

Available online at www.sciencedirect.com
SCIENCE DIRECT®

Polyhedron 22 (2003) 2661–2667

POLYHEDRON

www.elsevier.com/locate/poly

Synthesis, characterization and magnetic properties of a dinuclear complex $[Cu(2,2'\text{-bpy})(HL)(L)]_2(NO_3)_2\cdot(H_2O)_{3/2}$ and a 1D chain $\{[Cu(2,2'\text{-bpy})(4,4'\text{-bpy})_{1/2}(L)](ClO_4)\cdot(1/2H_2O)\}_n$ (L is *p*-aminobenzoate)

Da-Hua Hu [a], Wei Huang [a], Shao-Hua Gou [a,*], Jiang-Lin Fang [a], Hoong-Kun Fun [b]

[a] *State Key Laboratory of Coordination Chemistry, Nanjing University, Nanjing 210093, China*
[b] *X-ray Crystallography Unit, School of Physics, Universiti Sains Malaysia, 11800 USM, Penang, Malaysia*

Received 1 April 2003; accepted 12 May 2003

Abstract

Copper(II)-directed self-assembly led to a dinuclear complex and a 1D chain with empirical formula $[Cu(2,2'\text{-bpy})(HL)(L)]_2(NO_3)_2\cdot(H_2O)_{3/2}$ (**1**) and $\{[Cu(2,2'\text{-bpy})(4,4'\text{-bpy})_{1/2}(L)]\ (ClO_4)\cdot(1/2H_2O)\}_n$ (**2**) (L is *p*-aminobenzoate), respectively. X-ray single crystal structural analyses indicated that the $[Cu_2(2,2'\text{-bpy})_2(L)_2]$ unit was present in both compounds. The geometry of each copper(II) ion in the two compounds is distortedly pyramidal, where two nitrogen atoms from one 2,2′-bpy and two oxygen atoms from two different *p*-aminobenzoate constitute the pyramidal base, and one nitrogen atom of *p*-aminobenzoic acid (**1**) or 4,4′-bipyridine (**2**) takes the apical position. In **2**, a 1D polymeric chain, the separation of two copper(II) ions bridged by two different *p*-aminobenzoate ligands is 3.084 Å, and the distance to the adjacent copper(II) ion bridged by 4,4′-bpy moieties is 11.379 Å. The magnetic behavior of both compounds has been investigated.

Keywords: Copper(II) complexes; Self-assembly; Structural elucidation; Magnetic properties

1. Introduction

A great deal of interest in self-assembly of coordination complexes with specific frameworks is expanding rapidly in view of their potentially useful magnetic [1], catalytic [2] and nonlinear optical properties [3]. The structural topology of coordination complexes can be deliberately designed according to the coordination geometry of the chosen metal center and the structure of organic ligands. By combining transition metal ions, such as Zn^{2+}, Co^{2+}, Ni^{2+}, Pd^{2+}, Ag^{+}, Cu^{+}, Cu^{2+}, with bi- or multi-dentate organic ligands, 1D, 2D and 3D coordination frameworks including helicates, [4] diamondoids [5], T-shapes [6], ladders [7], square or rectangular grids [8] and octahedral structures [9] have been obtained. In general, transition metal ions serving as connectors are tetrahedral or octahedral in configuration [10], and organic ligands are rigid and multifunctional [11]. By now, complexes containing two different ligands, such as pyrazine and 4,4′-bipyridine [12], pyridine-4-carboxylate and 4,4′-bipyridine [13], phthalate (or terephthalate) and 4,4′-bipyridine [14], 4-hydroxybenzoate and 4,4′-bipyridine [15], have been amply documented.

Recently, we have undertaken a systematic investigation on five-coordinate copper(II) directed self-assembly. In our research, 2,2′-bipyridine has been used first to serve as a protective ligand to occupy two coordination sites of a naked copper(II) ion, then *p*-aminobenzoate has been applied as a bridging ligand to link two adjacent copper(II) atoms forming a dimeric unit, and finally suitable bi- or multi-dentate bridging ligands containing N- or O-donors, such as 4,4′-bpy, terephthalate, pyrazine, pyridine-4-carboxylate, are utilized to connect the resulting dimeric unit. Herein reported are a

---

* Corresponding author. Tel.: +86-25-359-5068; fax: +86-25-331-4502.
E-mail address: sgou@netra.nju.edu.cn (S.-H. Gou).

0277-5387/03/$ - see front matter © 2003 Elsevier Ltd. All rights reserved.
doi:10.1016/S0277-5387(03)00368-1

dinuclear complex $[Cu_2(2,2'\text{-bpy})_2(HL)_2L_2](NO_3)_2\cdot(H_2O)_{3/2}$ (**1**) and a 1D chain complex $\{[Cu(2,2'\text{-bpy})(4,4'\text{-bpy})_{1/2}(L)](ClO_4)\cdot(1/2H_2O)\}_n$ (**2**) (L is *p*-aminobenzoate), of which the crystal structures, spectroscopic and magnetic properties are studied.

2. Experimental

2.1. Physical measurements

Elemental analyses were measured with a Perkin–Elmer 240C analyzer. The infrared spectra were recorded with a Nicolet 5DX FT-IR spectrophotometer on KBr disks. Electrospray ionization mass spectra were recorded on a Finnigan MAT SSQ 710 mass spectrometer in a scan range 300–1200 amu. Magnetic susceptibilities of the complexes were measured using an Oxford Maglab 2000 magnetometer in the temperature range 2–280 K with an applied field of 1000 G. Diamagnetic corrections were estimated from Pascal's constants. EPR spectra were obtained on a Varian E9 spectrometer at the X-band frequency (9.7 GHz) at room temperature.

$[Cu(2,2'\text{-bpy})(NO_3)_2]\cdot 3H_2O$ was prepared according to the literature method [16], and 4,4′-bipyridine and *p*-aminobenzoic acid were purchased commercially. All other solvents and reagents were of analytical grade and used without further purification.

2.2. Syntheses

2.2.1. $[Cu(2,2'\text{-bpy})(HL)(L)]_2(NO_3)_2\cdot(H_2O)_{3/2}$ (*1*)

p-Aminobenzoic acid (0.17 g, 1.26 mmol) in methanol (25 cm^3) was added to a stirred solution of $[Cu(2,2'\text{-bpy})(NO_3)_2]\cdot 3H_2O$ (0.25 g, 0.63 mmol) in water (10 cm^3), and then the mixing solution was adjusted to pH 8.0 by addition of 4 mol l^{-1} NaOH solution. After the mixture was refluxed for 2 h and cooled to room temperature, dark-green micro-crystals were collected and washed with methanol and dried in a vacuum. Yields: (77%). *Anal*. Calc. for $C_{48}H_{43}N_{10}O_{15.5}Cu_2$: C, 50.75; H, 3.79; N, 12.33. Found: C, 50.55; H, 4.05; N, 12.39%. FT-IR: ν (cm^{-1}): 3459m, 3363m, 1686w, 1602m, 1584s, 1384s, 1018m. ES-MS: *m/z* 355 (100%) $[Cu(2,2'\text{-bpy})(L)]^+$.

2.2.2. $\{[Cu(2,2'\text{-bpy})(4,4'\text{-bpy})_{1/2}(L)](ClO_4)\cdot(1/2H_2O)\}_n$ (*2*)

Complex **2** was prepared by refluxing $[Cu(2,2'\text{-bpy})(NO_3)_2]\cdot 3H_2O$ (0.25 g, 0.63 mmol) with 4,4′-bpy (0.1 g, 0.63 mmol) and sodium *p*-aminobenzoate (0.10 g, 0.63 mmol) in methanol (50 cm^3) for 2 h. The mixture was cooled to room temperature, and then sodium perchlorate (0.098 g, 0.63 mmol) in methanol (5 cm^3) was added. Dark-green crystalline solids appeared immediately and were collected and dried in a vacuum. Yields: (85%). *Anal*. Calc for $C_{17}H_{14}ClN_3O_{6.5}Cu$: C, 44.01; H, 3.02; N, 9.06. Found: C, 44.07; H, 3.03; N, 8.98%. FT-IR: ν (cm^{-1}): 3415m, 3330m, 1624s, 1604s, 1397m, 1094s, 623m. ES-MS: *m/z* 282 (68%) $[Cu(2,2'\text{-bpy})(NO_3)]^+$.

2.3. Crystal structure determination and refinement of the structure

Crystal data of **1** and **2** were measured on a Bruker SMART CCD area detector at 293(2) K using graphite mono-chromated Mo Kα radiation ($\lambda = 0.71073$ Å). The intensities were reduced by using the program SAINT [17], and empirical absorption correction was done with the SADABS [18] program. The structure was solved by direct methods and refined by the least-squares method on F^2_{obs} using the SHELXTL-PC [19] software package. Hydrogen atoms were inserted in the calculated positions (C–H, 0.96 Å, N–H, 0.90 Å), while hydrogen

Table 1
Crystal data and details of the structure determination of **1** and **2**

Compound	1	2
Empirical formula	$C_{48}H_{45}N_{10}O_{15.5}Cu_2$	$C_{22}H_{18}ClN_4O_{6.5}Cu$
Formula weight	1137.02	541.39
Crystal size (mm)	0.3 × 0.2 × 0.2	0.24 × 0.20 × 0.14
Crystal system	monoclinic	orthorhombic
Wavelength (Mo Kα) (Å)	0.71073	0.71073
Space group	$P2_1/c$	*Imma*
a (Å)	20.065(1)	20.631(1)
b (Å)	13.394(1)	14.463(1)
c (Å)	19.125(1)	15.389(1)
β (°)	101.467(1)	90
V (Å^3)	5037.5(6)	4592.0(3)
Z	4	8
D_{calc}, (Mg m^{-3})	1.499	1.566
F(0 0 0)	2340	2208
μ (mm^{-1})	0.924	0.984
θ Range (°)	1.84–28.03	1.65–25.00
Temperature (K)	293(2)	293(2)
h_{min}/h_{max}	−26/26	−24/24
k_{min}/k_{max}	−15/17	−17/10
l_{min}/l_{max}	−18/24	−18/18
Reflections collected/unique	30 684/11 560	12 816/2178
Refinement method	full-matrix least-squares on F^2	full-matrix least-squares on F^2
Absorption correction	empirical	empirical
Data/parameters	11 560/732	2178/171
Final *R* indices [$I > 2\sigma(I)$]	$R_1 = 0.0501$, $wR_2 = 0.1525$	$R_1 = 0.0726$, $wR_2 = 0.1869$
R indices (all data)	$R_1 = 0.0723$, $wR_2 = 0.1599$	$R_1 = 0.0978$, $wR_2 = 0.2031$
Goodness-of-fit on F^2	1.063	1.042
Max./min., $\Delta\rho$ (e Å^{-3})	1.238/−0.531	0.969/−0.941

atoms from water molecules were located from difference maps. The experimental details and refinement results for **1** and **2** are listed in Table 1 and selected bond lengths and angles of **1** and **2** are given in Table 2.

3. Results and discussion

3.1. Crystal structures

X-ray single crystal structural analyses indicated that the [Cu$_2$(2,2′-bpy)$_2$(L)$_2$] unit is present in both **1** and **2**. Each copper(II) ion in [Cu$_2$(2,2′-bpy)$_2$(L)$_2$] unit is pyramidal, where two nitrogen atoms from one 2,2′-bpy and two oxygen atoms from two different *p*-aminobenzoate constitute the pyramidal base, and one nitrogen atom from *p*-aminobenzoic acid (**1**) or 4,4′-bipyridine (**2**) takes the apical position. The separation between two adjacent copper(II) ions bridged by the carboxyl group of *p*-aminobenzoate is 3.030 Å (**1**) or 3.084 Å (**2**) (Fig. 1).

In the crystal of **1**, the amino group of *p*-aminobenzoic acid is mono-coordinated to the central copper(II) ion at the axial position, and the bridging carboxyl group of *p*-aminobenzoate is bidentately bonded to two adjacent copper(II) ions, forming a dinuclear complex. The C–O bond lengths from the same *p*-aminobenzoate are slightly different, and the measured values are 1.262(4) Å [O(3)–C(28)], 1.264(4) Å [O(4)–C(28)], 1.271(4) Å [O(5)–C(35)] and 1.258(4) Å [O(6)–C(35)]. The basal plane of a pyramid is composed of N(3), N(4), O(4), O(6) and Cu(1), the bond distances of Cu(1)–N(3), Cu(1)–N(4), Cu(1)–O(4), Cu(1)–O(6) are 2.002(3), 1.990(3), 1.942(2) and 1.950(2) Å, respectively. The dihedral angle between the basal plane and the phenyl ring of *p*-aminobenzoic acid is 26.6°, and that between the phenyl rings of two different bridging *p*-aminobenzoates is 106.8°. In addition, the apical phenyl rings from two different *p*-aminobenzoic acids are twisted with a small dihedral angle of 9.9° and stretched along opposite directions.

In the dimeric complex, the traditional hydrogen bonds are present between the hydrogen atoms of the amino group and the carboxylic group of adjacent *p*-aminobenzoic molecules (Table 3). The N–H···O distances are 3.27 Å [N(5)–H(5A)···O(2)] and 2.89 Å [N(8)–H(8A)···O(8)]. With this kind of N–H···O hydrogen bonds, a 1D chain has come into being along the *c*-axis (Fig. 2). Furthermore, non-traditional C–H···O hydrogen bonds are also observed.

In the crystal structure of **2**, the [Cu$_2$(2,2′-bpy)$_2$(L)$_2$] units are linked by 4,4′-bpy ligands forming an infinite 1D polymeric chain (Fig. 3). The bridging carboxylate group of the *p*-aminobenzoate is bidentately bonded to two copper(II) ions and all C–O bond lengths are equal (1.263 Å), in contrast to those of in **1**. The pyridine rings in the 4,4′-bpy molecule make a dihedral angle of 12.6°. The dihedral angle between the basal plane, formed by O(1), N(1), O(1A), N(1A) and Cu(1), and the pyridine ring of 4,4′-bpy is 95.5°, and the bond lengths of Cu(1)–N(1), Cu(1)–N(1A), Cu(1)–O(1) and Cu(1)–O(1A) are 2.033(4), 2.033(4), 1.933(3) and 1.933(3) Å, respectively. It is interesting that the bond distances of Cu(1)–N(1) and Cu(1)–O(1) are similar to those reported for copper(II) complexes previously [20], but Cu(1)–N(2) (2.236 Å) is significantly longer than the usual pyridyl nitrogen to copper distance of 2.045 Å [21].

The traditional hydrogen bonds between the amino group of *p*-aminobenzoate and the perchlorate anion, and the non-traditional hydrogen bonds between the latter and the methylene group of 2,2′-bpy have been observed in **2**. As listed in Table 3, the bond distance of N–H···O and C–H···O are in the range 3.1052–3.3941 Å and 3.0463–3.3522 Å, respectively. It is noticed that the neighboring polymeric chains are arrayed in a 2,2′-bpy to 2,2′-bpy manner, and the plane–plane distance of 2,2′-bpy between adjacent chains is ca. 3.5 Å, which is

Table 2
Selected bond distances (Å) and angles (°) for **1** and **2**

1			
Cu(1)–O(4)	1.942(2)	Cu(2)–N(2)	2.001(3)
Cu(1)–O(6)	1.950(2)	Cu(2)–N(1)	2.003(3)
Cu(1)–N(5)	2.325(3)	Cu(1)–Cu(2)	3.0303(6)
Cu(1)–N(4)	1.990(3)	O(3)–C(28)	1.262(4)
Cu(1)–N(3)	2.002(3)	O(4)–C(28)	1.264(4)
Cu(2)–O(5)	1.935(2)	O(5)–C(35)	1.271(4)
Cu(2)–O(3)	1.952(2)	O(6)–C(35)	1.258(4)
Cu(2)–N(8)	2.295(3)		
O(4)–Cu(1)–O(6)	90.8(1)	O(5)–Cu(2)–O(3)	90.6(1)
O(4)–Cu(1)–N(5)	94.5(1)	O(5)–Cu(2)–N(8)	94.0(1)
O(6)–Cu(1)–N(5)	91.7(1)	O(3)–Cu(2)–N(8)	96.6(1)
O(3)–C(28)–O(4)	124.7(3)	O(6)–C(35)–O(5)	123.9(3)
O(4)–Cu(1)–N(4)	168.7(1)	O(5)–Cu(2)–N(2)	95.1(1)
O(6)–Cu(1)–N(4)	92.9(1)	O(3)–Cu(2)–N(2)	167.5(1)
O(4)–Cu(1)–N(3)	93.6(1)	O(5)–Cu(2)–N(1)	169.2(1)
O(6)–Cu(1)–N(3)	169.2(1)	O(3)–Cu(2)–N(1)	91.9(1)
N(4)–Cu(1)–N(3)	81.1(1)	N(2)–Cu(2)–N(1)	80.6(1)
N(4)–Cu(1)–N(5)	96.1(1)	N(2)–Cu(2)–N(8)	94.1(1)
N(3)–Cu(1)–N(5)	97.8(1)	N(1)–Cu(2)–N(8)	96.2(1)
2			
Cu(1)–O(1)	1.933(3)	C(8)–C(8B) [a]	1.493(1)
Cu(1)–N(1)	2.013(4)	Cl(1)–O(2)	1.344(7)
Cu(1)–N(2)	2.236(6)	Cl(1)–O(3)	1.344(7)
O(1)–C(9)	1.263(4)		
		O(1)–Cu(1)–N(2)	91.9(2)
O(1)–Cu(1)–O(1A) [b]	90.9(2)	O(1)–C(9)–O(1C) [c]	123.6(6)
O(1)–Cu(1)–N(1)	169.3(2)	O(2)–Cl(1)–O(3D) [d]	119.1(2)
N(1)–Cu(1)–N(1A) [b]	80.3(3)		
N(1)–Cu(1)–N(2)	97.6(2)		

[a] $-x+1, -y-1/2, z$.
[b] $-x+1, y, z$.
[c] $x, -y+1/2, z$.
[d] $-x+1/2, y+0, -z+1/2$.

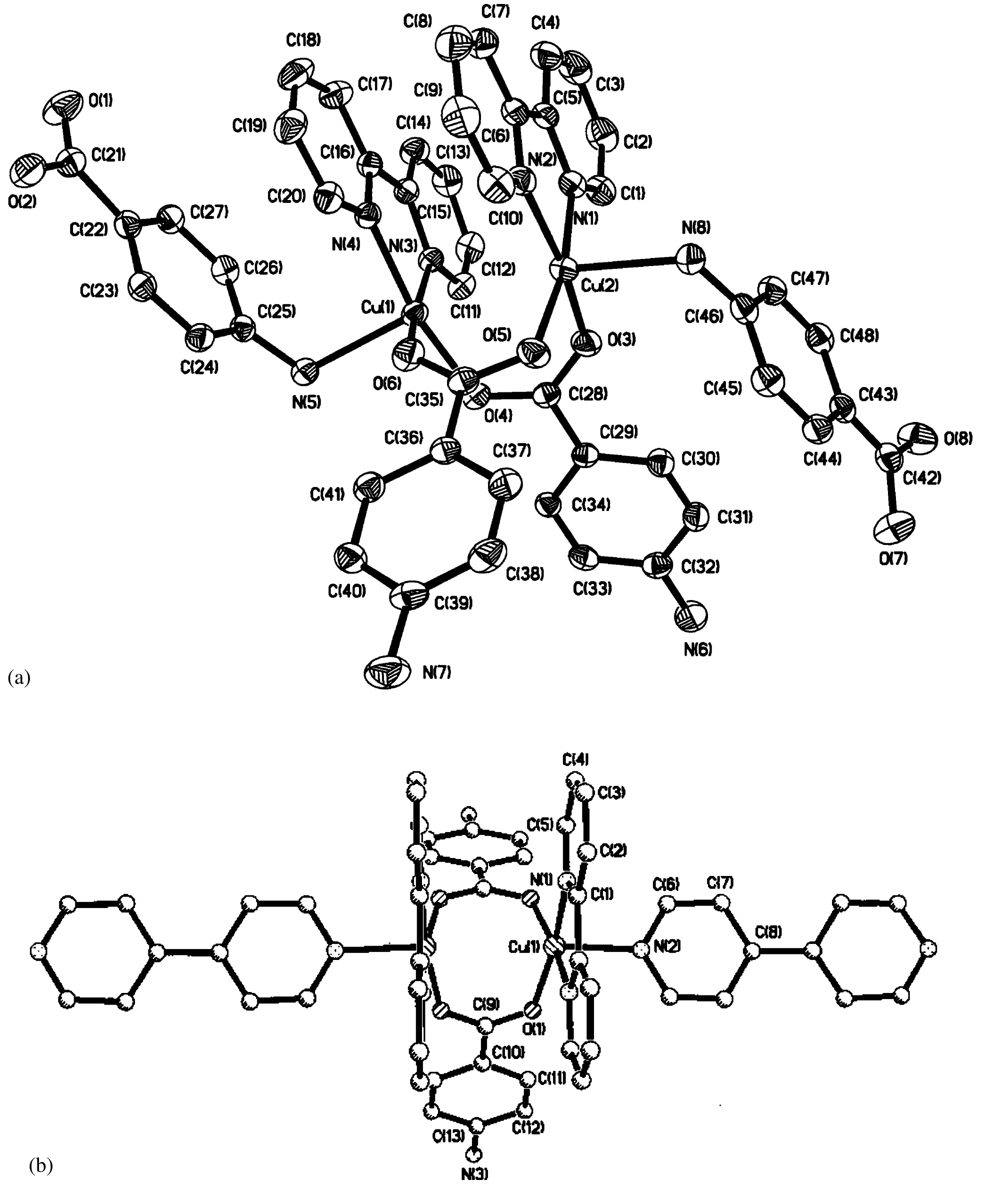

Fig. 1. ORTEP drawing (30% probability) of the coordination sphere of the copper atom and atom numbering scheme of **1** (a) and **2** (b).

less than that within a single chain, ca. 3.8 Å. All planes of 2,2′-bpy are nearly coplanar with a small dihedral angle of 7.5°. Apparently, there are π–π interactions between these neighboring chains. The hydrogen bonds and π–π interactions in **2** generate a 3D network where four oxygen atoms of a perchlorate anion acts as bridges to link adjacent [Cu(2,2′-bpy)(4,4′-bpy)(L)] units (Fig. 4).

3.2. Magnetic properties

The molar magnetic susceptibilities of **2** in the range 2–300 K exhibit strong temperature dependence (Fig. 5(b)). The maximum occurs around 45 K, and the minimum is around 11 K. As the structure described, the system is an alternating magnetic exchange chain, whose Hamilton can be expressed as $H = -2J\Sigma(S_{i-1}S_i + \alpha S_iS_{i+1})$ $(\alpha < 1)$. The study of Bonner et al. [22] indicates that magnetic susceptibilities of alternative chains with $S = 1/2$ for all values of α will show a broaden maximum and decrease exponentially while $T \to 0$. The $\chi - T$ plot has a similar pattern for the broaden maximum but magnetic susceptibilities increase again when the temperature falls below 11 K. Therefore, the behavior below 11 K is not the consquence of alternative intrachains but arises from the contributions of two possibilities. One is the exchange coupling of the interchain, and the other is the presence of a small amount of non-polymerized copper(II) ions, exhibiting paramagnetism, as impurities in the powder sample. Based on the analytical expression of Hatfield [23], a practical formula can be used for this case:

Table 3
Hydrogen bonding (Å, ^{O}) in complex **1** and **2**

D–H···A	D–H	H–A	D···A	∠DHA
1				
O(1W)–H(1WB)···O(1) [a]	0.8492	2.1452	2.8155	135.62
O(2W)–*H(2WB)···O(23) [b]	0.8705	2.3658	3.0150	131.61
O(2)–H(20)···O(1W) [c]	0.8457	1.7684	2.5843	161.48
N(5)–H(5A)···O(2) [d]	0.8806	2.4275	3.2706	160.44
N(5)–H(5B)···O(11) [e]	0.9064	2.0831	2.9586	162.03
N(7)–H(7B)···O(1W) [f]	0.8988	2.4345	3.2859	158.17
N(8)–H(8A)···O(8) [g]	0.8914	2.0244	2.8909	163.72
C(4)–H(4A)···O(22) [h]	0.9300	2.5337	3.4433	165.94
2				
C(3)–H(3A)···O(2)	0.9630	2.3542	3.2736	159.50
C(5)–H(5A)···O(3) [i]	0.9632	2.5085	3.3522	146.23
C(5)–H(5A)···O(1) [j]	0.9632	2.5324	3.0463	113.42
O(1W)–H(1WA)···O(3) [k]	0.7903	2.2990	3.0303	154.26
O(1W)–H(1WA)···O3 [l]	0.7903	2.2990	3.0303	154.26
N(3)–*H(3B)···O(2) [m]	0.9025	2.5860	3.3941	149.39
N(3)–*H(3B)···O(2) [n]	0.9025	2.2456	3.1052	159.04

[a] $x, 3/2-y, -1/2+z$.
[b] $x, 1/2-y, 1/2+z$.
[c] $1-x, 3/2+y, 1/2-z$.
[d] $1-x, -1/2+y, 1/2-z$.
[e] $1-x, 1/2+y, 1/2-z$.
[f] $1-x, 1-y, -z$.
[g] $-x, 1/2+y, 1/2-z$.
[h] $x, 3/2-y, 1/2-z$.
[i] $x, -y, 1-z$.
[j] $1-x, y, z$.
[k] $x, 1/2+y, 1-z$.
[l] $1/2-x, 1/2+y, 1/2+z$.
[m] $1-x, y, 1+z$.
[n] $1/2+x, y, 3/2-z$.

$$\chi = (1-p)\frac{g^2\beta^2}{3k\left(T\frac{z'J'}{3k}\right)}\,\frac{A+Bx+Cx^2}{1+Dx+Ex^2+Fx^3}+p\frac{c}{T} + \chi_{\mathrm{TIP}}$$

Here $z'J'/3k$ represents the interchain magnetic coupling; p is the percent of monomer or impurities in the powder sample, $x = J/kT$; the A–F coefficients are functions of α; χ_{TIP} is the temperature independent paramagnetism.

A good fit by a least-square method gives $J = -72.2$ K; $\alpha = 0.034$; $\chi_{\mathrm{TIP}} = 0.00069$; $p = 2.2\%$, $z'J'/3k = -1.25$ K, $c = 0.4$ while the g factor is fixed at 2.28 from a room temperature EPR spectrum. The minor positive value of α means that the coupling for alternative bridges are both antiferromagnetic interactions but quite different. In view of the structure, it is understood that the magnetic coupling via the 4,4′-bipy ligand will be much weaker than that via p-aminobenzoic anions since two pyridine rings in 4,4′-bipy bridges are long and p-aminobenzoic bridges are triplicate. This also agrees with the EPR signal that shows a typical dimeric copper(II) pattern at room temperature. The value $z'J'/3k = -1.25$ K implies that interchain magnetic coupling is also a very weak antiferromagntic interaction.

The molar magnetic behavior of **1** in the range 5–300 K is very similar to **2** (Fig. 5(a)), revealing strong antiferromagnetic coupling between pairs of copper(II) centers. Below 16 K a paramagnetic tail appears too, exhibiting that some monomer impurities are mixed in the compound. Hence, the magnetic susceptibilities per Cu ion may be fitted using the modified Bleaney–Bowers expression [24]:

$$\chi = (1-p)\frac{Ng^2\beta^2}{kT}\,\frac{1}{3+\mathrm{e}^{-2J/kT}}+p\frac{Ng^2\beta^2}{4kT}$$

where $2J$ is the energy gap between single and triple states and the other parameters have their usual meaning. The result shows $2J = -117$ K, $p = 2.3\%$, and $g = 2.034$. The antiferromagnetic exchange coupling in the dimer is significantly larger than that in the chain compound since there are fewer interactions with the adjacent molecules.

4. Supplementary materials

Crystallographic data (excluding structural factors) for the structures of **1** and **2** have been deposited with the Cambridge Crystallographic Data Center with the CCDC No. 173870 and 163855, respectively. Copies of the data can be obtained free of charge on application to CCDC, 12 Union Road, Cambridge CB2 1EZ, UK (fax: +44-1223-336033; e-mail: deposit@ccdc.cam.ac.uk or www: http://www.ccdc.cam.ac.uk).

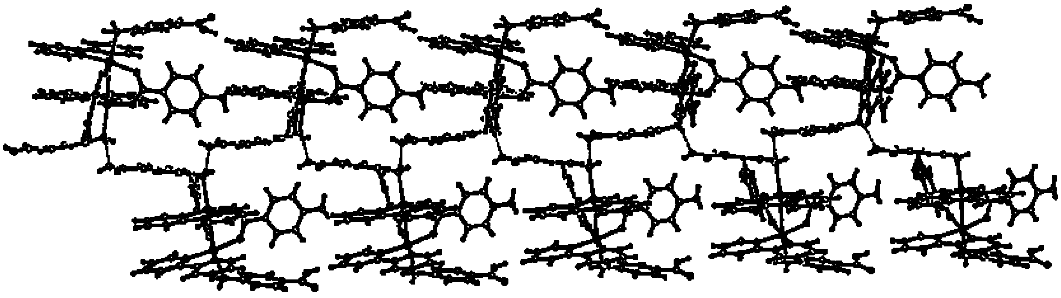

Fig. 2. View of the 1D chain structure of **1** along the c-axis.

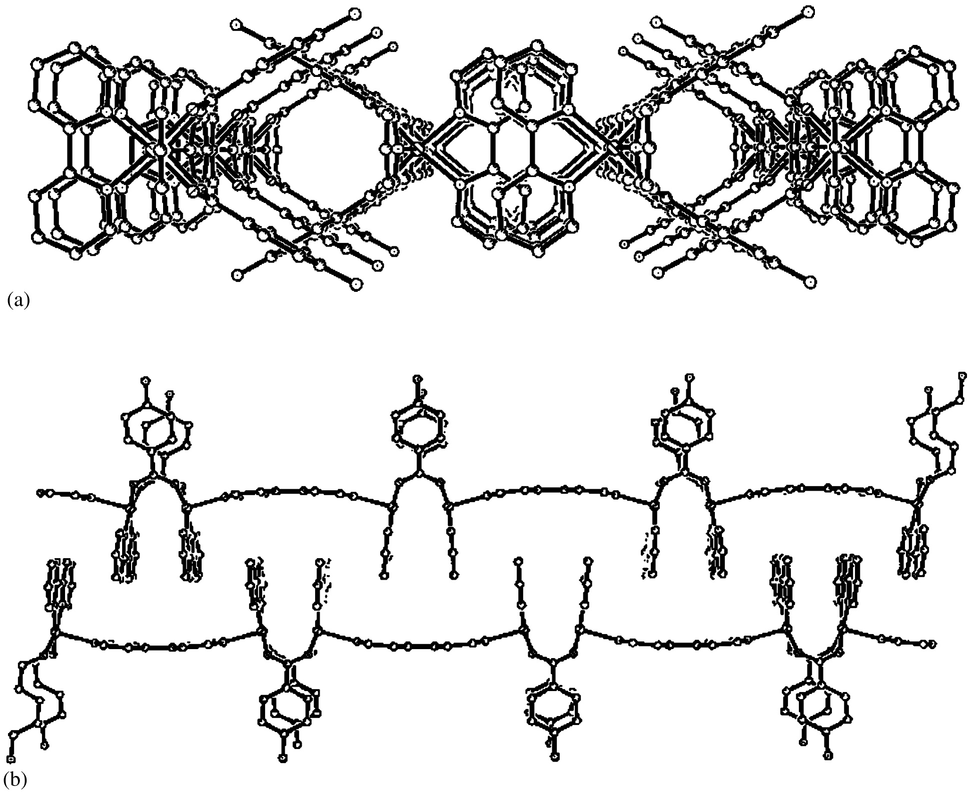

Fig. 3. 1D chain structure of **2**, top view (a) and side view (b).

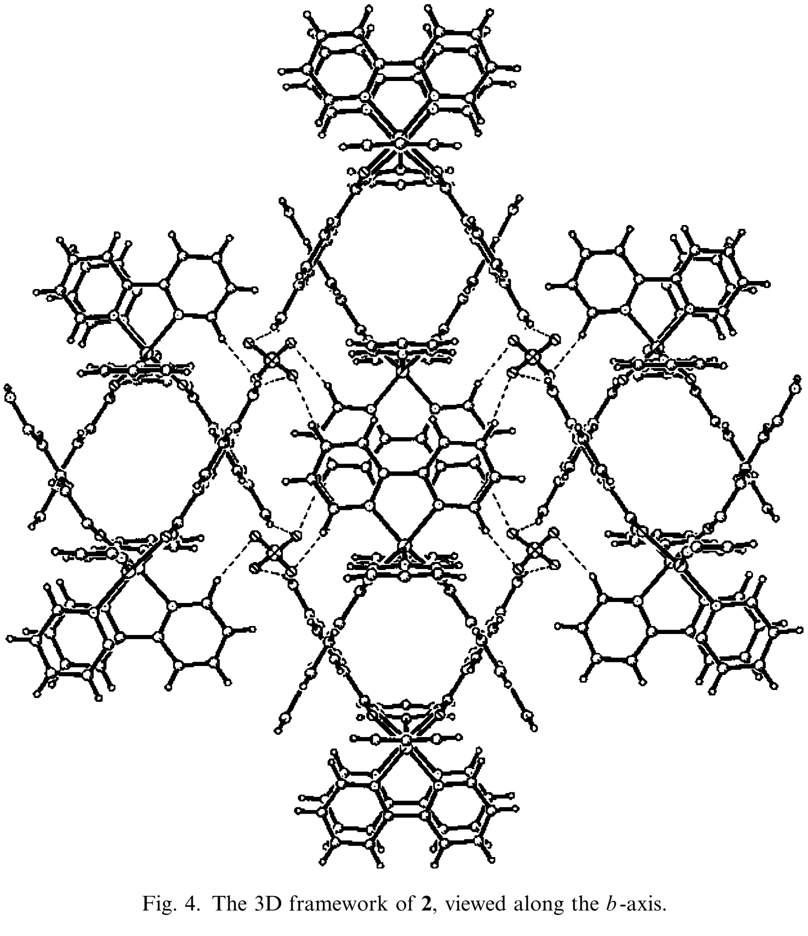

Fig. 4. The 3D framework of **2**, viewed along the *b*-axis.

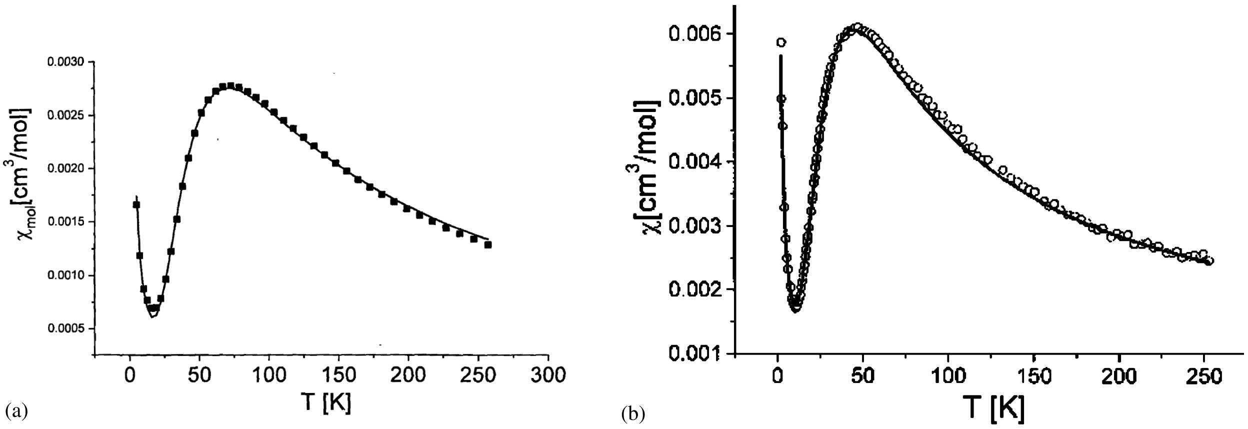

Fig. 5. Temperature dependence of χ_{mol} (o) of **1**(a) and **2**(b). Solid curves are based on the theoretic calculation and dotted lines represent the experimental values.

Acknowledgements

We thank the Jiangsu Science and Technology Department (BK2001031) and the Third World Academy of Sciences (TWAS) for their financial support. This work is also partly funded by the National Natural Science Foundation of China (project 20271026). W. H. is grateful to the Nanjing University Talent Development Foundation.

References

[1] (a) J.O. Charles, L.K. Cheryl, J.M. Richard, M.T. Louis, Inorg. Chem. 21 (1982) 64;
(b) R.E. Del Sesto, A.M. Arif, J.S. Miller, Inorg. Chem. 39 (2000) 4894.

[2] M. Fujita, Y.J. Kwon, S. Washizu, K. Ogura, J. Am. Chem. Soc. 116 (1994) 1151.

[3] O.R. Evans, R.-G. Xiong, Z. Wang, G.K. Wong, W. Lin, Angew. Chem., Int. Ed. Engl. 38 (1999) 536.

[4] K. Biradha, C. Seward, M.J. Zaworotko, Angew. Chem., Int. Ed. Engl. 38 (1999) 492.

[5] O.M. Yaghi, H. Li, J. Am. Chem. Soc. 117 (1995) 10401.

[6] (a) O.M. Yaghi, H. Li, J. Am. Chem. Soc. 118 (1996) 295;
(b) H. Gudbjartson, K. Biradha, K.M. Poirier, M.J. Zaworotko, J. Am. Chem. Soc. 121 (1999) 2599.

[7] (a) W. Huang, S. Gou, D. Hu, C. Suchada, H.-K. Fun, Q. Meng, Inorg. Chem. 40 (2001) 1712;
(b) M. Fujita, Y.J. Kwon, Y.O. Sasaki, K. Yamaguchi, K.J. Ogura, J. Am. Chem. Soc. 117 (1995) 7287;
(c) O.M. Yaghi, H. Li, T.L. Groy, Inorg. Chem. 36 (1995) 4292;
(d) L. Carlucci, G. Ciani, D.M. Proserpio, Chem. Commun. (1999) 449.

[8] C.V.K. Sharma, R.D. Rogers, Chem. Commun. (1999) 83.

[9] S. Subramanian, M.J. Zaworotko, Angew. Chem., Int. Ed. Engl. 34 (1995) 2127.

[10] A. Van, A. Gerard, E.Q.-C. Maria, M. Ilpo, T. Urho, R. Jan, Inorg. Chim. Acta 298 (2000) 221.

[11] (a) C. Lucia, C. Gianfranco, M.P. Davide, R. Silvia, Chem. Commun. (2000) 1319;
(b) C. Lucia, C. Gianfranco, M.P. Davide, S. Angelo, J. Am. Chem. Soc. 117 (1995) 4562.

[12] M.-L. Tong, X.-M. Chen, X.-L. Yu, C.W.M. Thomas, J. Chem. Soc., Dalton Trans. (1998) 5.

[13] L.R. MacGillivray, R.H. Groeneman, J.L. Atwood, J. Am. Chem. Soc. 120 (1998) 2676.

[14] J. Tao, M.-L. Tong, X.-M. Chen, J. Chem. Soc., Dalton Trans. (2000) 3669.

[15] M.-L. Tong, H.-J. Chen, X.-M. Chen, Inorg. Chem. 39 (2000) 2235.

[16] G. Eugenio, M. Giovanni, S. Daniele, S.-E. Liliana, Inorg. Chim. Acta 299 (2000) 253.

[17] Siemens, SAINT v4 Software Reference Manual, Siemens Analytical X-Ray Systems, Inc., Madison, WI, USA, 1996.

[18] G.M. Sheldrick, SADABS, Program for Empirical Absorption Correction of Area Dectector Data, University of Göttingen, Germany, 1996.

[19] Siemens, SHELXTL, Version 5 Reference Manual, Siemens Analytical X-Ray Systems, Inc., Madison, WI, USA, 1996.

[20] R.E. Sesto, A.M. Arif, J.S. Miller, Inorg. Chem. 39 (2000) 4094.

[21] S. Kitagawa, S. Kawata, M. Kondo, Y. Nozaka, M. Munakata, Bull. Chem. Soc. Jpn 66 (1993) 3387.

[22] J.C. Bonner, H.W. Blöte, J.W. Bray, I.S. Jacobs, J. Appl. Phys. 50 (1979) 1810.

[23] J.W. Hall, W.E. Marsh, R.R. Weller, W.E. Hatfield, Inorg. Chem. 20 (1980) 10330.

[24] R. Gupta, S. Mukheriee, R. Mukheriee, J. Chem. Soc., Dalton Trans. (1999) 4025.